Energetics of Non-Covalent Interactions from Electron and Energy Density Distributions

Gabriele Saleh[a,*], *Carlo Gatti*[b,c], *Leonardo Lo Presti*[b,c,d]

[a] Moscow Institute of Physics and Technology, 9 Institutskiy Lane, Dolgoprudny, Moscow Region, 141700, Russia

[b] Istituto di Scienze e Tecnologie Molecolari del CNR (CNR-ISTM), Via Golgi 19, 20133 Milano (Italy)

[c] Center for Materials Crystallography, Aarhus University, Langelandsgade 140, DK-8000 Aarhus C. Denmark

[d] Università degli Studi di Milano, Dipartimento di Chimica, Via Golgi 19, 20133 Milano (Italy)

gabriele.saleh@unimi.it, c.gatti@istm.cnr.it, leonardo.lopresti@unimi.it

(*) CORRESPONDING AUTHOR FOOTNOTE : : gabriele.saleh@unimi.it, tel. +7 4987446524, fax: +7 4954084254

ABSTRACT

Non-covalent interactions dictate how molecules interact with their surroundings. Enhancing their knowledge is crucial to explain phenomena of utmost importance like self-assembly, chemical reactivity and crystallization. In this work, the possibility of investigating Non-Covalent Interactions (NCIs) by using the Reduced Density Gradient (RDG) in tandem with energy densities descriptors is explored. A sample of 30 molecular adducts, spanning dispersive, hydrogen bonds and X-H···π interactions was considered. Potential relationships among molecule···molecule Stabilization Energies and energy densities were sought for. Adducts characterized by NCIs having similar physical origins exhibit an excellent linear correlation between Stabilization Energies and kinetic energy densities integrated over the volume enclosed by low-value RDG isosurfaces. Estimating stabilization energies this way is computationally unexpensive and applicable also to electron densities derived from experiment, where a reliable approximation to the kinetic energy density in the intermolecular regions is afforded through Abramov's functional. Potential energy densities, when averaged over the basins enclosed by low-value RDG isosurfaces, assume different values according to the kind of interaction class (dispersive, HBs, X–H···π, and so on). This observation provides a new recipe to disentangle how the various NCIs contribute to the total Stabilization Energy. Implications on the possibility of retrieving quantitative thermodynamic information from the topology of suitable scalar fields are discussed.

Keywords: Non-covalent interactions, reduced density gradient, electron density, energy densities, stabilization energy

1. INTRODUCTION

Non-Covalent Interactions (NCIs) are essential in most biochemical processes [1] representing the working principle through which all organisms -from bacteria to human beings- operate. NCIs are also in the heart of key chemical processes such as molecular crystals formation [2] and self-assembly [3]. Investigating NCIs through quantum mechanics has always been a challenge for theory [4], but also a way to complement the information coming from their experimental study. Quantum models may indeed provide insights on the physical mechanisms behind the formation of the various kinds of NCIs [4]. Moreover, computed potential energy surfaces are convenient tools to develop force fields able to predict the behavior of biochemical systems by means of molecular dynamics [5].

The Stabilization Energy (SE) -*i.e.* the energy gain when a molecular dimer is formed [4]- plays a fundamental role in the study of NCIs. It provides a measure of the interaction strength and so ranks the possible conformations of supramolecular structures according to their thermodynamic stability [6]. This approach has the well-known drawback of requiring a very high level of theory to be reliable [4], so that it becomes prohibitively expensive even for medium-size molecular pairs. Conversely, the so-called Quantum Chemical Topology (QCT) approaches have in the last decades become increasingly popular for exploring chemical interactions [7], including NCIs. As a general definition, QCT embodies all those techniques which are based on the dynamical systems theory and aimed at extracting chemical insight from the analysis of suitable scalar fields. For example, the Quantum Theory of Atoms in Molecules ('QTAIM' [8–10]) focuses on the analysis of the Electron Density (ED) scalar field and provides a quantum-mechanically rooted definition of chemical paradigms such as bonds and atoms. A quantitative link between QCT and SE would bring two main advantages. It would provide useful information in the quest

for systematically improving the accuracy of exchange-correlation functionals of the Density Functional Theory (DFT), especially if the link is built with scalar fields commonly employed in DFT (*e.g.* the ED). Moreover, it could enhance both the interpretive and predictive capabilities of QCT approaches by endowing them with a quantitative link to thermodynamic.

Several efforts have been spent in the attempt of extracting information on the NCI energetics from the topology of the ED distribution. Espinosa *et al.* [11,12] have shown that kinetic and potential energy densities, evaluated at the (3,-1) ED critical points [8] of the D-H···A Hydrogen Bonds (HBs) bear an empirical relationship with the H···A distance and, indirectly, with the dissociation energy. Their analysis covered a number of gas-phase dimers and molecular crystals; for A = O a correlation between energy densities and the interaction potential of the molecular dimers was also obtained [13]. Similarly, Contreras-Garcia and Wang [14] were able to mimic the shape of the potential energy surface of a given dimer by integrating its "signed" ED over the Reduced Density Gradient (RDG) isosurfaces, defined in section 2.1. The ED local sign was taken equal to that of the second eigenvalue of the ED Hessian matrix in their study. Alonso *et al*. [15] found a rough proportionality between the interaction energy and both the volume and the electron charge enclosed into the RDG isosurfaces of dimers bound by various kinds of dispersive interactions,

This work is aimed at finding relationships between QCT and SE potentially applicable to all classes of NCIs. We consider the correlation between SE and several quantities integrated over the volume enclosed by the RDG isosurfaces associated to NCIs. In particular, we focus on the possibility of investigating NCIs by means of the combined use of RDG and energy densities. 30 molecular dimers were analysed as test cases, spanning very different kinds of directional and non-directional NCIs, namely: HBs, X-H···π (where X is an electron withdrawing fragment) and

dispersive interactions. We will show that, for groups of systems sharing the same kind of NCI type, a linear correlation exists between SE and the kinetic energy density integrated over the space enclosed by RDG isosurfaces. An overview of the quantities scrutinized in this work is given in the next session, whereas the test cases and the adopted theoretical method are sketched out in section 3. Results are presented and discussed in section 4, whereas section 5 concludes and overviews future perspectives.

2 THEORETICAL BACKGROUND

2.1 THE REDUCED DENSITY GRADIENT AND ITS ISOSURFACES

RDG (eq. 1) relies on the mathematical construction of the so-called 'generalized gradient approximation' of the DFT exchange-correlation functional, defined using RDG as independent variable [16]. Although it can not be associated to a precise quantum mechanical meaning, RDG is yet generally considered as a measure of the inhomogeneity of the ED distribution. Moreover, as noted by Zupan *et al*. [17] and later explored in details by Johnson *et al.* [18], low-RDG values are associated with the onset of chemical interactions. The expression of RDG is

$$s(\mathbf{r}) = \frac{1}{2(3\pi^2)^{\frac{1}{3}}} \frac{|\nabla\rho(\mathbf{r})|}{\rho(\mathbf{r})^{4/3}} \quad (1),$$

where s(**r**) is the RDG and ρ(**r**) the ED. Johnson *et al*. [18] showed that low-value RDG isosurfaces appear among interacting atoms, regardless of the nature of their interaction. When only low ED regions are considered, the occurrence of these isosurfaces is associated to NCIs. This property of RDG was exploited to build the so-called 'NCI descriptor' [18]. The latter allows one to characterize NCIs by mapping on these RDG isosurfaces the quantity $\rho(\mathbf{r})\text{sign}\lambda_2$, where λ_2 is the second eigenvalue of the ED Hessian matrix. The sign of λ_2 was used to distinguish between

attractive ($\lambda_2<0$) and repulsive interactions ($\lambda_2>0$). The ED, instead, was exploited to rank the strength of NCIs.

A close parallelism exists between the appearance and shape of RDG isosurfaces and several topological QTAIM features of ED. Saleh *et al*. [19] considered in details analogies and differences between the 'NCI descriptor' and QTAIM approaches, with particular focus on using experimentally-derived EDs [19,20]. Here we just remind that low-RDG isosurfaces always appear wherever a critical point -*i.e.* a point where $\nabla\rho(\mathbf{r})$ vanishes- is present (eq.1) and that the use of RDG isosurfaces enables one to recover the delocalized character of certain NCIs. In this way, problems arising from the localized description of interactions. inherent to QTAIM, can be partly overcome. The reader is referred to refs. 19 and 20 for a deeper discussion on this topic.

2.2 KINETIC, POTENTIAL AND TOTAL ENERGY DENSITIES

The total, kinetic and potential energy densities (hereinafter generically termed 'energy densities') are extensively used in QTAIM to characterize chemical interactions. Their values at bond critical points provide a powerful tool to discriminate between covalent and non-covalent interactions [21]. While there is no unique definition for the energy densities, several expressions have been proposed yielding the corresponding energy for the system when integrated over the whole space. A widely used [8,21] definition of kinetic energy density is the following:

$$\mathrm{G}(\mathbf{r}) = \frac{1}{2}\sum_{i=1}^{N} \alpha_i |\nabla\varphi_i(\mathbf{r})|^2 \qquad (2),$$

where the sum runs over all occupied natural orbitals φ_i, α_i being their occupation number. Regarding the potential energy density, the local form of the virial theorem [8] is customarily used to evaluate such quantity in a computationally inexpensive way:

$$V(\mathbf{r}) = \frac{1}{4}\nabla^2\rho(\mathbf{r}) - 2G(\mathbf{r}) \quad (3).$$

Rigorously speaking, the quantity evaluated through eq. 3 is the virial field at **r,** representing the effective potential field felt by an electron at **r** and providing a short range description for the potential energy density [22]. The total energy density at **r** is then given by:

$$H(\mathbf{r}) = G(\mathbf{r}) + V(\mathbf{r}) \quad (4).$$

3 METHODS

3.1 CHOICE OF TEST CASES

As anticipated in the Introduction, this work is aimed at exploring the correlation between SE and quantities integrated over the space enclosed by the low-value RDG isosurfaces associated to intermolecular interactions, *i.e.* those located between the interacting molecules. To this end we selected relatively simple molecular dimers which mainly interact through one specific kind of NCI. Such dimers were taken from refs 23,24 and 25, where very accurate geometries (MP2/cc-pVTZ) and SE (CCSD(T)/complete basis) were obtained[1,2]. For hydrogen bonds, we considered several donors (C, O, F) and acceptor (O, N, F) atoms, thereby ensuring that our results may be applicable to a wide range of HB types. Regarding the choice of adducts representing the class of dispersive interactions, we selected dimers formed by hydrocarbons (including both aromatic and aliphatic fragments) where induction and electrostatic effects are known to be negligible compared to those due to dispersion [26]. The X-H···π interactions, where X is an electron-withdrawing

[1]We found that a more favorable energy minimum exists on the potential energy surface for the HF···MeOH pair. Therefore, we re-optimized this dimer at the MP2/cc-pVTZ level of theory and evaluated the SE at the CCSD(T)/cc-pVQZ level (Counterpoise method for basis set superposition error correction was also applied).

[2] A HCN···C_2H_4 dimer was also added to the X-H···π set of interactions. The starting geometry was similar to that of the C_2H_2···C_2H_4 adduct. Geometry optimization and SE evaluation were both carried out at the same level of theory as for the HF···MeOH dimer.

fragment, were also examined as a quite challenging case. They are, characterized by an important dispersive contribution and, yet, share many features with HBs [27]. Note that CH_4···benzene was considered as a dispersive rather than an X-H···π interaction, according to refs.23 and 27.

3.2 THEORETICAL CALCULATIONS, EVALUATION OF RDG AND ENERGY DENSITIES AND INTEGRATION PROCEDURE

When not otherwise specified, the calculations were carried out at the B3LYP/cc-pVTZ level of theory using the code GAUSSIAN 09 [28]. Geometries were kept frozen at the ones reported in the literature. The evaluation of all scalar fields considered in this work and their integration inside the RDG isosurfaces was performed with the 'NCImilano' code [29], except for the energy densities (Eq. 2-4) whose integration was afforded using a modified version of such program. In particular, the integration inside the volume bounded by a certain isosurface was carried out by producing a grid of points which encloses the isosurface and applying the following formula:

$$A(RDG_\delta) = \sum_{i(RDG<\delta)} A(\mathbf{r}_i) l_X l_Y l_Z \quad (5),$$

where $A(RDG_\delta)$ is the integral of the quantity A over the space enclosed by the δ-isosurface, $A(\mathbf{r}_i)$ is the value of such quantity at the (grid) point $\mathbf{r}_i$ and l_X,l_Y and l_Z are the grid step sizes in the x, y, and z directions, respectively. Orthogonal grids were used throughout. The summation is carried out on all grid points $\mathbf{r}_i$ having RDG<δ. The grid step sizes adopted vary from 0.015 to 0.025 bohr for HBs and from 0.02 to 0.05 bohr for the other systems. We checked for some representative cases the convergence of integrated quantities with respect to the grid step size: we found that lowering the grid step size below 0.04 for HB dimers and 0.06 for the other systems results in negligible differences (<0.5%) in the integrated quantities.

Isosurfaces having a δ value comprised in the range 0.3-0.6 are commonly employed for the investigation of NCIs [14,18,19,20]. In this work we considered isosurfaces having δ=0.5. The stability of our results against the use of different δ values was verified (see *infra*).

4 RESULTS AND DISCUSSION

4.1 ON THE REDISTRIBUTION OF ELECTRON AND ENERGY DENSITIES

In general, when two molecules are brought from infinite distance to their equilibrium one, their geometries relax and their ED distributions rearrange. To investigate the electronic effects, we calculated the interaction density[3] for a few representative dimers, three of which are shown in Fig. 1a-c. We observe that for HB and O-H···π interactions there is a (slight) accumulation of charge in the region between the two fragments, while the opposite is true for NCIs dominated by dispersive forces. In general, it can be seen that the rearrangement of ED distribution due to NCIs takes place mainly within the monomers, the ED changes in the intermolecular region being comparatively much smaller (as already noted in ref. 30). In other words, the perturbation on the wavefunction of each monomer due to induction effects (and, to a much lesser extent, to dispersion and higher order terms in the language of perturbation theory [31]) barely affects the intermolecular ED. Therefore, one can conclude that the ED distribution in the intermolecular region is mostly shaped by the tiny overlap of the electron clouds of the monomers. As a consequence, the factor primarily responsible for the ED distribution in the intermolecular region

[3] The interaction density is defined as the distribution of ρ(**r**)[dimer]-ρ(**r**)[monomers], where ρ(**r**)[dimer] is the ED distribution of the dimer, whereas ρ(**r**)[monomers] is the superposition of ED distribution of the two isolated monomers at the geometry they have in the dimer. The same procedure is applied to evaluate the interaction energy density.

is the geometry of the dimer, which is determined in turn by the forces pulling the molecules at the equilibrium distance. When energy density rearrangements are considered (Fig. 1d-i), the changes in the intermolecular regions relative to those in the intramolecular ones are even smaller than for the ED distribution, hence the same considerations hold true. In general, an increase of the kinetic energy density between the two interacting molecules is observed, as expected when two closed-shell fragments approach each other (see, for example, ref. 32). Such increase, however, is overridden by a decrease of potential energy density, leading to a (slightly) negative value of total interaction energy density and to an overall stabilization of electrons in the intermolecular regions.

4.2 CORRELATION BETWEEN STABILIZATION AND KINETIC ENERGIES

In Fig.2 the plot of SE *vs* $G(RDG_{0.5})$ (eq. 5) values of the investigated dimers is displayed. For the purpose of a qualitative discussion, Fig. 2 also shows the energy densities mapped onto low-value RDG isosurfaces associated to NCIs[4] for some representative cases. First, we note that HBs -even the weak ones- are characterized by values of G(**r**) and V(**r**) significantly higher than other interaction types. Isosurfaces associated to weak HBs display positive values of H(**r**). On passing from weak to moderate HBs, G(**r**) increases more than |V(**r**)| does, leading to higher positive values of H(**r**). By moving from moderate to strong HBs, however, |V(**r**)| increases more steeply than G(**r**) and as a result such HBs are characterized by negative H(**r**) in the intermolecular region. On the contrary, dispersive interactions are denoted by very low and positive H(**r**) values, which result from small and comparable G(**r**) and |V(**r**)| contributions, with G(**r**) being invariably slightly greater than |V(**r**)|. As expected [27], the G(**r**) and H(**r**) values for X-H···π interactions lie somehow

[4] To single out only the RDG isosurfaces associated with NCIs, RDG was calculated solely for those regions having ED<0.08 e/a.u.. Note that this practice of plotting a quantity on RDG isosurfaces associated to NCIs is the same as reported in ref. 18

in between those for dispersive interactions and HBs. We also note that the isosurfaces associated with ring critical points (here seen at the center of benzene rings) display a greatly positive H(**r**) value, resulting from a very high, destabilizing G(**r**) contribution. This evidence complies with the interpretation drawn from the 'NCI descriptor' [18,33], *i.e*. that these kinds of isosurfaces represent the steric crowding associated with ring closure.

Correlation of SE against G($RDG_{0.5}$) values, exhibits a remarkable linear trend for HBs and dispersive interactions (Fig. 2). For these latter, the result is not completely unexpected, since the dispersive interaction strength is known to be proportional to the number of close atom-atom contacts, or equivalently to the area of overlap between molecular surfaces [34, 35]. Indeed, a very good linear correlation with SE can be attained even by simply considering the volume enclosed by the 0.5 RDG isosurfaces. For example, the correlation coefficient using the volume is R^2=0.992, to be compared with R^2=0.998 obtained from the linear regression against G($RDG_{0.5}$) (Figures S1-S3 in the Supporting Information)[5]. Conversely, the linear correlation found for HB dimers has a less straightforward origin. At odd with what observed for hydrocarbons, for HB systems the linear SE/G($RDG_{0.5}$) trend cannot be simply ascribed to changes in the isosurfaces volume or in the intermolecular G(**r**) value. This is demonstrated in Fig. S4 and S5, where SE is plotted against the average G(r) inside the isosurfaces and against the isosurfaces volume. The plots show that the linear correlation results from the combined effect of both the volume change and the G(**r**) variation and no evident correlations can instead be observed between G($\mathbf{r}_{BCP}$) (or, similarly, G(**r**) averaged over RDG isosurface) and SE (Fig. S6) .However, a closer inspection of our results reveals this is the case for the G(**r**) averaged over RDG isosurface when the examined HBs share

[5] Note that similar results -namely a linear trend for interaction energy *vs* RDG isosurfaces volume- were obtained by Alonso *et al*. (Fig. S3 of ref. [15]) for a series of dimers of aromatic molecules

the same acceptor atoms (Fig. S4-S5). We also observe that for dimers having similar SE values, such averaged G(**r**) values decrease in the order X-H···N>X-H···O>X-H···F.[6] The opposite trend is found when the volume of RDG isosurfaces is considered. The compensation between these two inverse tendencies results in the nearly perfect linear correlation between SE and the $G(RDG_{0.5})$ values shown in Figure 2. Besides that *vs* $G(RDG_{0.5})$, a roughly linear trend can be found for SE also *vs.* other quantities, namely $H(RDG_{0.5})$, $V(RDG_{0.5})$ and $\rho(RDG_{0.5})$. Nevertheless, only the SE *vs.* $G(RDG_{0.5})$ regression exhibits an R^2 value very close to 1. This seems to be a general observation: for all the interaction types here considered, the best correlation with SE was obtained against the kinetic energy density values integrated within the RDG isosurfaces.

The SE-$G(RDG_{0.5})$ correlation, however, breaks down when HB dimers involving atoms of different periods are considered (*e.g.* $HCl\cdots MeNH_2$, HCl···MeOH and HBr···MeOH). This may be due either to the fact that orbitals with higher principal quantum number come into play or to the increasing importance of dispersive forces when heavy atoms are considered. This aspect, along with the exploration of other possible correlation schemes for sets of HB dimers involving atoms of different periods, will be further investigated in forthcoming works.

Regarding X-H···π interactions, no straightforward correlations were found between SE and $G(RDG_{0.5})$ values. Indeed, while dispersive interactions and HBs share a similar interaction mechanism, the same does not hold true for X-H···π interactions. For the latter, the dispersion, polarization and electrostatic terms provide very different relative contributions to the SE, depending on the nature of the X fragment [27]. However, a closer inspection reveals that the X-H···π dimers may be divided into two main groups which do separately show a linear trend of SE

[6]It should be noted that our test case set of 10 HB dimers can be divided according to the acceptor atom type as follow: oxygen (5 dimers), nitrogen (4 dimers), fluorine (1 dimer). As the trend here discussed concerns a small sample of test cases, it may not have universal significance.

vs $G(RDG_{0.5})$ (Fig. 2). Such division bears a precise chemical significance, as it separates dimers bearing strong electron-withdrawing X atoms from the weaker-bearing ones. These latter give rise to NCIs characterized by a significant dispersive contribution to SE, whereas in the former dimers the interaction is characterized by a mechanism more similar to that of HBs, where electrostatic and induction contributions play the dominant role [27]. This difference is clearly reflected in the slope of SE *vs* $G(RDG_{0.5})$ lines, which are closer to those of hydrocarbons when the dispersive contribution is dominant, and closer to those of HBs for the interactions which are more HB-like.

Assessment of the accuracy of the established correlation against the chosen RDG isovalues and the quality of the wavefunction can be found in the Supporting Information (Section S III).

One of the most appealing applications of the approach we propose is the possibility of evaluating the interaction energy in molecular crystals from their experimentally-derived ED distributions. For many of such systems the evaluation of the ED distribution from accurate X-ray diffraction experiments can nowadays be obtained on an ordinary basis [36], and the molecular geometry determined from such experiments is known to be very precise [37]. However, the $G(\mathbf{r})$ distribution is not accessible from the ED distribution only. To overcome this limitation, we implemented in our code 'NCImilano' the possibility of evaluating the energy densities in terms of the approximated ED-based functional introduced by Abramov [29,38]. Such functional, which is known to closely reproduce[7] $G(\mathbf{r})$ in intermolecular regions [39,40], was tested against its ability in mimicking also the linear correlation observed in Fig. 2. As expected, an excellent agreement was found between the value of $G(RDG_{0.5})$ evaluated from the wavefuntion and that obtained using the Abramov's functional (Figures S7-S9). Consequently, the conclusions drawn above about the

[7] By reproducing $G(\mathbf{r})$, we mean that a distribution close to that obtained using the exact formula given in Eq. 2 is derived

linear correlation between SE and $G(RDG_{0.5})$ values hold true also when such functional is employed. This evidence paves the way towards using our approach to accurately evaluate SE from experimentally-derived ED distributions. Such a goal will however imply a further level of complexity in the close-packed crystalline environments, due to possible ambiguities in disentangling individual molecule···molecule interactions.

4.3 AVERAGE POTENTIAL ENERGY DENSITY AS A TOOL TO CLASSIFY DIFFERENT CLASSES OF INTERACTIONS

In order to assess the suitability of the present approach in estimating SEs, a rigorous method to establish which interaction type a given isosurface belongs to is called for. While qualitative classification can be done by mapping energy densities onto the RDG isosurfaces (see Section 4.2 above), the value of $V(\mathbf{r})$ averaged in the volume bounded by RDG isosurfaces was found to provide a more quantitative way to distinguish the various interactions. Such quantity represents the potential felt by electrons and, as such, it is expected to be high in the intermolecular regions for the interactions dominated by electrostatic forces and to be there small when the forces holding molecules together are nothing but dispersion. A histogram plot of such values for the 30 dimers considered in this work is reported in Fig. 3. It can be clearly seen that HBs, dispersive and X-H···π interactions are characterized by different ranges of average $V(\mathbf{r})$ values. In addition, for the latter interactions, the distinction made above based on the electron-withdrawing character of the donor atom is neatly reflected in the value of the averaged $V(\mathbf{r})$. As interactions of a given kind span a quite large range of averaged $V(\mathbf{r})$ values, this may lead to a (small) overlap between different interaction types. Actually, for the systems considered here this happens only for the CH_4···benzene dimer, which displays an averaged $V(\mathbf{r})$ value higher than those covered by the dispersive interactions.

5 CONCLUSIONS AND FUTURE PERSPECTIVES

In this work we explored the possibility to investigate non-covalent interactions by using the reduced density gradient in tandem with energy densities. Our study was based on a sample of 30 molecular dimers each of which can be associated to one among the dispersive, hydrogen bonds or X-H···π types of non-covalent interaction. By analysing the redistribution of electron and energy densities that takes place upon the onset of non-covalent interactions, we confirmed that the main rearrangement of such densities occurs within the molecular fragments, the changes in the intermolecular regions being far less important. Moreover, mapping the energy density onto low-value RDG isosurfaces allows for distinguishing among the various kind of interactions, on the basis of well-distinguishable ranges of kinetic and potential energy densities.

The main advance of this work lies, however, in the possibility to recover the stabilization energy of the investigated molecular dimers from topological features of electron and energy density distributions. We have shown that for dimers whose non-covalent interactions have similar physical origin, an excellent linear correlation exists between the stabilization energy and the kinetic energy density integrated over the volume bounded by low-value Reduced Density Gradient isosurfaces. Such correlation is likewise retrieved when the kinetic energy density is evaluated through the functional introduced by Abramov, making our approach suitable for the estimation of the stabilization energy also from X-ray diffraction experiments. Clearly, its application to molecular crystals demands further tests to establish whether the stabilization energy can or can not be simply recovered from the additive contributions of a number of different isosurfaces associated to various types of NCIs. To this end, *in vacuo* model systems characterized

by more than one and possibly competing non covalent interactions should be included in a future analysis.

To have an unbiased criteria to establish the interaction type a given isosurface is associated to, we propose the use of the potential energy density averaged over the space enclosed by the isosurface. It was demonstrated that such quantity assumes different ranges of values for the different interaction types considered in our study.

The next step will be the extension of our approach to other NCI classes and to larger systems where more than one interaction type is involved in the energy stabilization. Since it is computationally inexpensive and not too dependent on the adopted theoretical level, such a generalized tool should allow to reliably determine the interaction energy also for those systems where the very accurate theoretical approaches required to estimate the stabilization energy [4] cannot yet be applied. Moreover, an estimation of the energy associated to intramolecular non-covalent interactions, where there is no unique way to define an interaction/stabilization energy, should also become viable this way.

Overall, the present study represents a step forward in the quest for retrieving the quantitative thermodynamic information embodied in the topology of quantum-mechanically rooted scalar fields like the electron density, one of the possible forms of the kinetic energy density and the virial density.

ACKNOWLEDGEMENTS

This work was supported by the grant of the Government of the Russian Federation (No. 14.A12.31.0003) and by the Danish National Research Foundation (DNRF93) through the Center for Materials Crystallography.

	angular coefficient (x 10^{-3})	Intercept (x 10^{-3})	R^2
HBs	1.35(1)	-2.0(1)	0.999
dispersive	5.22(8)	-1.3(2)	0.998
X-H···π (▲)	4.2(2)	-7.6(7)	0.995
X-H···π (●)	6.3(5)	-8(11)	0.982

Table 1. Equations obtained for the lines interpolating stabilization energy *vs* $G(RDG_{0.5})$. The second, third and fourth columns reports the angular coefficient, the intercept, and the correlation coefficient. Each row corresponds to a given interaction type, according to the discussion reported in sections 4.2 and 4.3. The two distinct groups of X-H···π interactions are labeled according to the symbols (in brackets) used in Figure 2 to denote them.

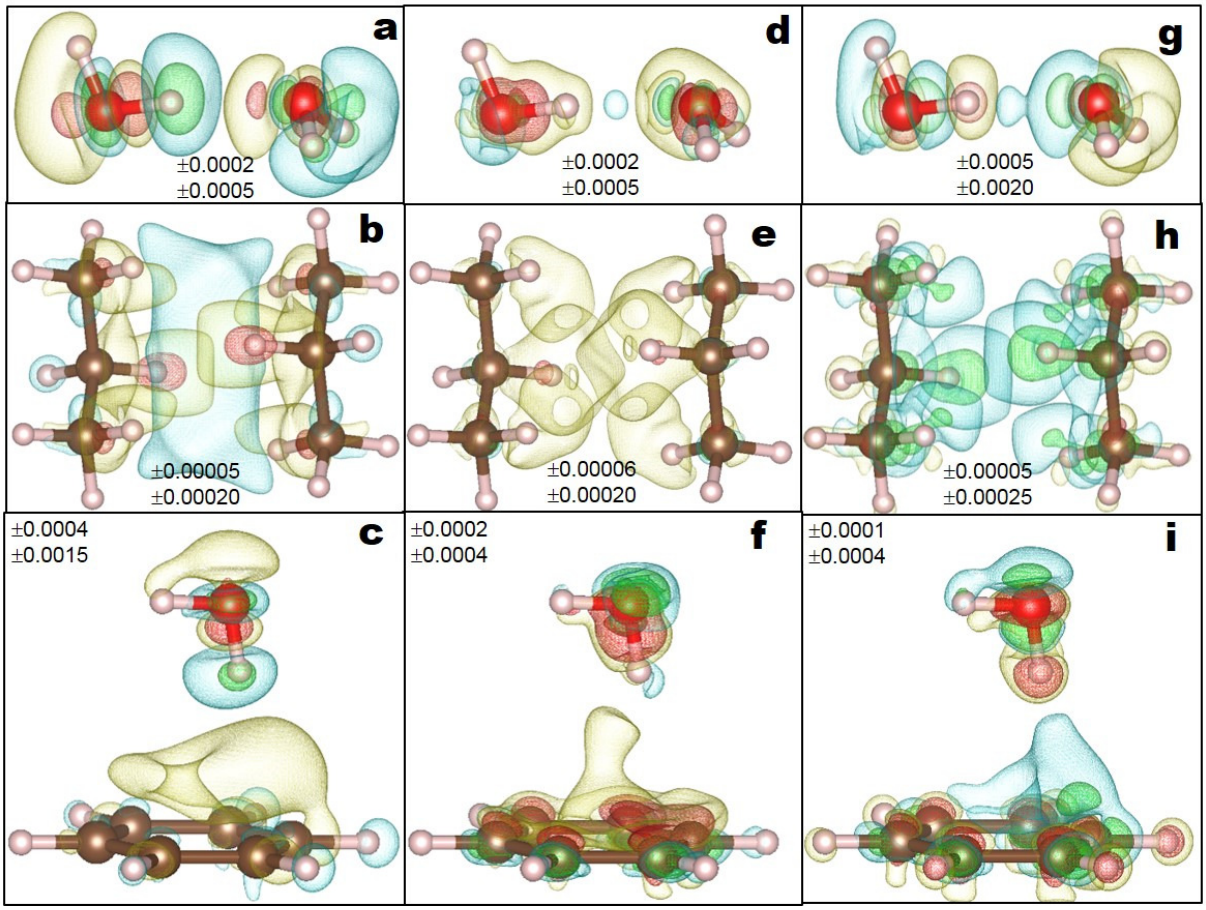

Figure 1. Isosurfaces representing the redistribution of ρ(**r**) (first column), G(**r**) (second column) and H(**r**) (third column) upon formation of molecular dimers. For each image, 4 isosurfaces are shown and their value is reported below (atomic units used throughout). The isosurfaces are colored from the most positive to the most negative in the following sequence: red-yellow-blue-green. All the images were obtained using the software VESTA [41]

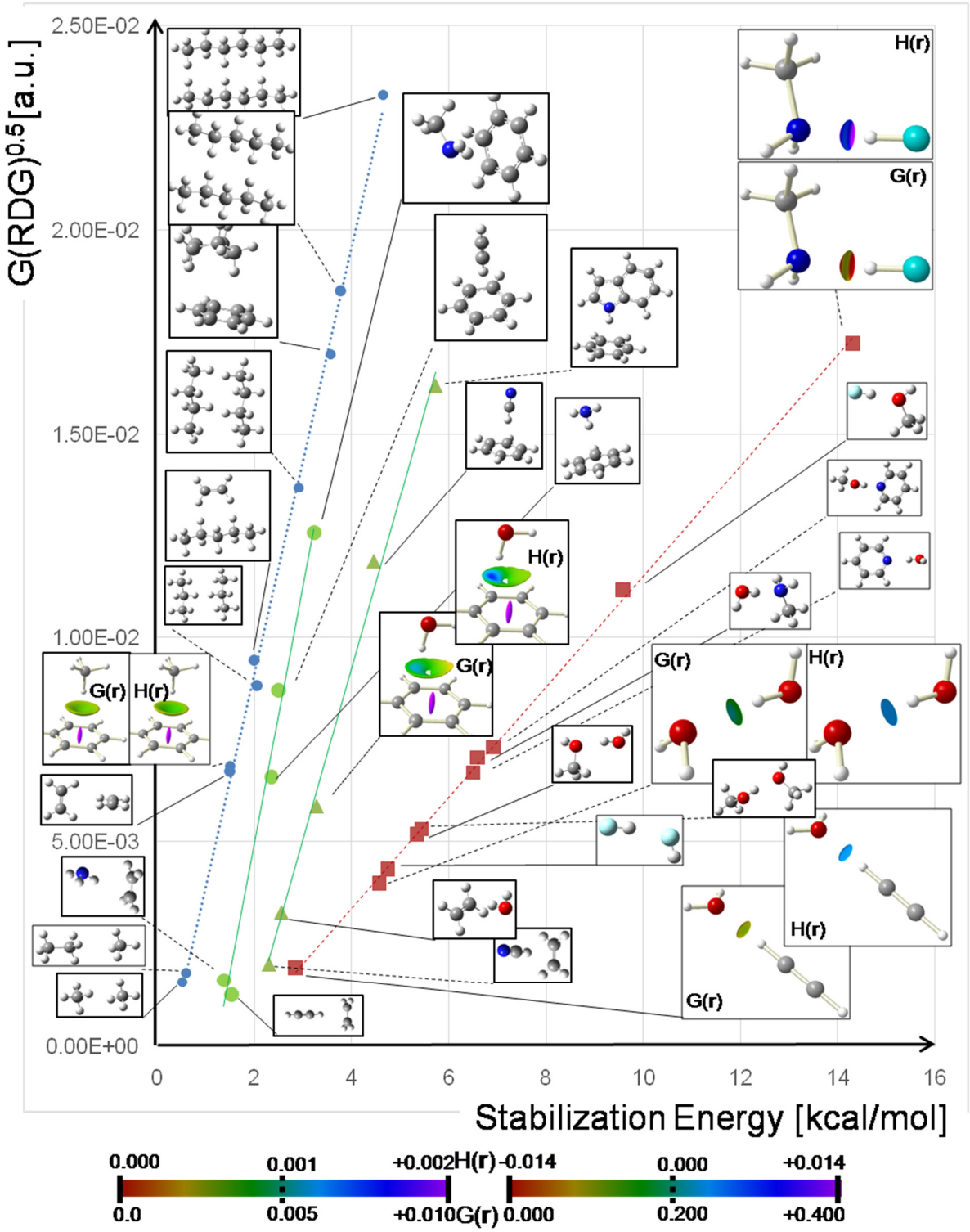

Figure 2. Plot of Stabilization Energy *vs* $G(RDG_{0.5})$ (see sections 1 and 3.2 for the definition of these quantities). The various points are colored according to their associated interaction type: blue, green and red colors were used for dispersive, X-H···π and HBs interactions, respectively. For X-H···π, different symbols (circles and triangles) denote their two distinct groups (see section 4.2). For some representative

dimers, G(**r**) and H(**r**) are mapped on the 0.5-RDG NCI isosurfaces, using an ED cutoff of 0.08 e/a.u. to single out only RDG isosurfaces associated to NCI, according to ref. 18). The color scales used for such images are reported at the bottom of the figure: the right one refers to HBs and the left one to the other interactions. For all remaining dimers, only the equilibrium structures are shown. Atoms colors: grey, white, blue, red, and azure for C, H, N, O and F, respectively. The equations and R^2 coefficients for each line are reported in Table 1. The isosurfaces plots were obtained using the software Moliso [42] and the structural images through Gaussview [28]

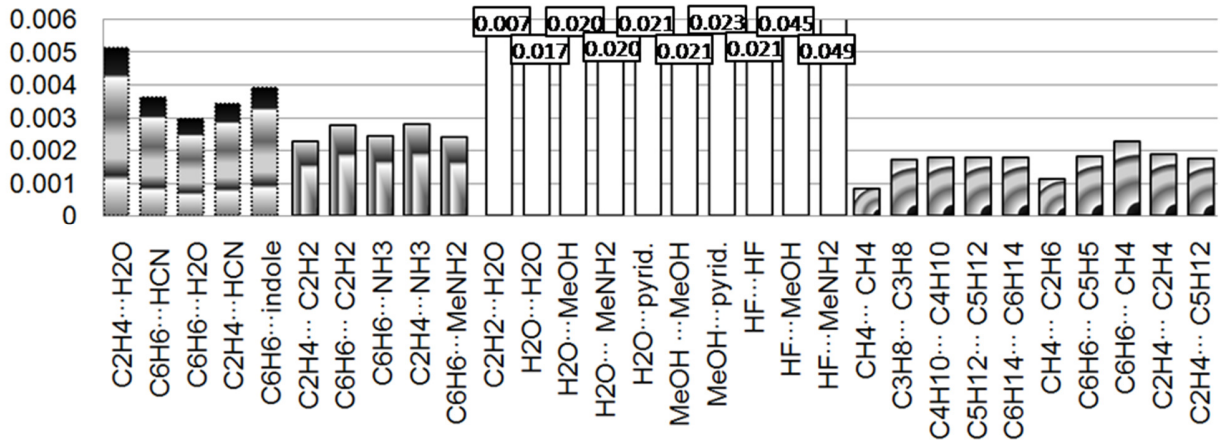

Figure 3. Histogram of V(**r**) averaged in the space bounded by the intermolecular 0.5 RDG isosurfaces for the dimers considered in the present study. For the interactions belonging to different types (according to the discussion reported in sections 4.2 and 4.3), the corresponding columns were filled with different motifs. Since HBs (empty columns) have values much higher than for other interactions, the corresponding columns were truncated and the value for each dimer is reported at the top of the column.

REFERENCES

[1] A. L. Lehninger, D. L. Nelson, M. M. Cox, Principles of Biochemistry, second edition, Worth Publishers Inc., New York, 1993.

[2] A. Gavezzotti, Molecular Aggregation. Structure Analysis and Molecular Simulation of Crystals and Liquids, IUCr monographs on Crystallography n. 19, Oxford University Press, Oxford (UK), 2007

[3] N. Krishnamoorthy, M.H. Yacoub, S.N. Yaliraki, A computational modeling approach for enhancing self-assembly and biofunctionalisation of collagen biomimetic peptides, Biomaterials 32 (2011) 7275–7285.

[4] K. Müller-Dethlefs, P. Hobza, Noncovalent Interactions: A Challenge for Experiment and Theory, Chem. Rev. 100 (2000) 143-167.

[5] C. D. Sherrill, B. G. Sumpter, M. O. Sinnokrot, M. S. Marshall, E. G. Hohenstein, R. C. Walker, I. R. Gould, assessment of Standard Force Field Models Against High-Quality Ab Initio Potential Curves for Prototypes of π–π, CH/π, and SH/π Interactions, J. Comput. Chem., 30 (2009) 2187-2193.

[6] J. Černý, P. Hobza, Non-covalent interactions in biomacromolecules, Phys. Chem. Chem. Phys. 9 (2007) 5291–5303.

[7] P. L. A. Popelier, Quantum Chemical Topology: on Bonds and Potentials, Struc. Bond. 115 (2005) 1–56.

[8] R.F.W. Bader, Atoms In Molecules: A Quantum Theory, Clarendon press, Oxford (UK), 1990.

[9] C. F. Matta, R. J. Boyd, The Quantum Theory of Atoms in Molecules. From SolidState to DNA and Drug Design, Wiley-VCH, Weinheim, (D) 2007.

[10] C. Gatti, Chemical Bonding in crystals: new directions, , Z. Kristallogr. 220 (2005), 399–457.

[11] E. Espinosa, E. Molins, C. Lecomte, Hydrogen bond strengths revealed by topological analyses of experimentally observed electron densities, Chem Phys. Lett. 285 (1998) 170-173.

[12] I. Mata, I. Alkorta, E. Molins, E. Espinosa, Universal Features of the Electron Density Distribution in Hydrogen Bonding Regions: A Comprehensive Study Involving H···X (X=H, C, N, O, F, S, Cl, π) Interactions, Chem. Eur. J. 16 (2010) 2442 – 2452.

[13] E. Espinosa, E. Molins, Retrieving interaction potentials from the topology of the electron density distribution: The case of hydrogen bonds, J. Chem. Phys. 113 (2000) 5686-5694.

[14] J. Contreras-García, W. Yang, E. R. Johnson, Analysis of hydrogen-bond interaction potentials from the electron density: Integration of NCI regions, J Phys Chem A, 115 (2011) 12983–12990.

[15] M. Alonso, T. Woller, F. J. Martín-Martínez, J. Contreras-García, P. Geerlings, F. De Proft, Understanding the Fundamental Role of π/π, σ/σ, and σ/π Dispersion Interactions in Shaping Carbon-Based Material, Chem. Eur. J. 20 (2014) 4931–4941.

[16] W. Koch, M. C. Holthausen A Chemist's Guide to Density Functional Theory, 2nd Edition, Wiley-vhc, Weinheim (D) , 2001.

[17] A. Zupan, K. Burke, M. Ernzerhof, J.P. Perdew, Distributions and averages of electron density parameters: Explaining the effects of gradient corrections, The Journal of Chemical Physics 106 (1997) 10184–10193.

[18] E.R. Johnson, S. Keinan, P. Mori-Sánchez, J. Contreras-García, A.J. Cohen, W. Yang, Revealing Noncovalent Interactions, J. Am. Chem. Soc. 132 (2010) 6498–6506.

[19] G. Saleh, C. Gatti, L. Lo Presti, J. Contreras-Garcia, Revealing Non-covalent Interactions in Molecular Crystals through Their Experimental Electron Densities, Chem. Eur. J. 18 (2012) 15523–15536.

[20] G. Saleh, C. Gatti, L. Lo Presti, Non-Covalent Interactions *via* the Reduced Density Gradient: Independent Atom Model versus Experimental Multipolar Electron Densities, Comp. Theor. Chem., 998. (2012) 148-163.

[21] P. Macchi, A. Sironi Chemical bonding in transition metal carbonyl clusters: complementary analysis of theoretical and experimental electron densities, Coordination Chemistry Reviews 238-239 (2003) 383-412.

[22] T. A. Keith, R. F. W. Bader, Y. Aray, Structural homeomorphism between the electron density and the virial field, Int. J. Quatum Chem. 57 (1996) 183–198.

[23]P. Jurečka, J. Šponer, J. Černý, P. Hobza, Benchmark database of accurate (MP2 and CCSD(T) complete basis set limit) interaction energies of small model complexes, DNA base pairs, andamino acid pairs, Phys. Chem. Chem. Phys. 8 (2006) 1985-1993.

[24] J. Řezáč, K. E. Riley, P. Hobza, S66: A Well-balanced Database of Benchmark Interaction Energies Relevant to Biomolecular Structures, J. Chem. Theory Comput., 7 (2011) 2427–2438.

[25] J. Granatier, M. Pitoňák, P. Hobza, Accuracy of Several Wave Function and Density Functional Theory Methods for Description of Noncovalent Interaction of Saturated and Unsaturated Hydrocarbon Dimers, J. Chem. Theory Comput. 8 (2012) 2282−2292.

[26] A. J. Bordner, Assessing the Accuracy of SAPT(DFT) Interaction Energies by Comparison with Experimentally Derived Noble Gas Potentials and Molecular Crystal Lattice Energies, ChemPhysChem 13 (2012) 3981 – 3988.

[27] M. Nishio, The CH/p hydrogen bond in chemistry. Conformation, supramolecules, optical resolution and interactions involving carbohydrates Phys. Chem. Chem. Phys. 13 (2011) 13873-13900.

[28] M. J. Frisch, G. W. Trucks, H. B. Schlegel, G. E. Scuseria, M. A. Robb, J. R. Cheeseman, G. Scalmani, V. Barone *et al*. Gaussian 09 (Revision A.1), 2009, Gaussian, Inc., Wallingford CT.

[29] G. Saleh, L. Lo Presti, C. Gatti, D. Ceresoli, NCImilano: an electron-density-based code for the study of noncovalent interactions, J. Appl. Cryst. 46 (2013) 1513-1517.

[30] C. Gatti, E. May, R. Destro, F. Cargnoni, Fundamental Properties and Nature of CH··O Interactions in Crystals on the Basis of Experimental and Theoretical Charge Densities. The Case of 3,4-Bis(dimethylamino)-3-cyclobutene-1,2-dione (DMACB) Crystal, J. Phys. Chem. A 106 (2002) 2707–2720.

[31] B. Jeziorski, R. Moszynski,K. Szalewicz, Perturbation Theory Approach to Intermolecular Potential Energy Surfaces of van der Waals Complexes, Chem. Rev. 94 (1994) 1887–1930.

[32] R. F. W. Bader, H. J. T. Prestson, The Kinetic Energy of Molecular Charge Distributions and Molecular Stability, Int. J. Quant. Chem., 3 (1969) 327-347.

[33] R. Chaudret, B. de Courcy, J. Contreras-Garcìa, E. Gloaguen, A. Zehnacker-Rentien, M. Mons, J.-P. Piquemal, Unraveling non-covalent interactions within flexible biomolecules: from electron density topology to gas phase spectroscopy, Phys. Chem. Chem. Phys. 16 (2014) 9876-9891.

[34] S. Tsuzuki, T. Uchimaru, M. Mikami, K. Tanabe High Level ab-Initio Calculations of Intermolecular Interaction of Propane Dimer: Orientation Dependence of Interaction Energy, J. Phys. Chem. A 106 (2002) 3867-3872.

[35] S. Tsuzuki, K. Honda, T. Uchimaru, M. Mikami Magnitude of Interaction between n-Alkane Chains and Its Anisotropy: High-Level ab-Initio Calculations of n-Butane, n-Petane, and n-Hexane Dimers J. Phys. Chem. A 108 (2004) 10311-10316.

[36] T. S. Koritsanszky, P. Coppens, Chemical Applications of X-ray Charge-Density Analysis, Chemical Reviews, 101 (2001) 1583–1628.

[37] See, for example: G. Saleh, R. Soave, L. Lo Presti, R. Destro, Progress in the Understanding of the Key Pharmacophoric Features of the Antimalarial Drug Dihydroartemisinin: An Experimental and Theoretical Charge Density Study, Chem. Eur. J. 19 (2013) 3490-3503.

[38] Y. A. Abramov, On the possibility of kinetic energy density evaluation from the experimental electron-density distribution, Acta Cryst. A53 (1997) 264-272.

[39] E. Espinosa, I. Alkorta, I. Rozas, J. Elguero, E. Molins, About the evaluation of the local kinetic, potential and total energy densities in closed-shell interactions, Chem. Phys. Lett. 336 (2001) 457–461.

[40] O. Galvez, P. C. Gomez, L. F. Pacios, Variation with the intermolecular distance of properties dependent on the electron density in hydrogen bond dimers, Chem. Phys. Lett. 337 (2001) 263–268.

[41] K. Momma F. Izumi, VESTA: a three-dimensional visualization system for electronic and structural analysis, J. Appl. Crystallogr. 41 (2008) 653-658.

[42] C.B. Hübschle, P. Luger, MolIso– a program for colour-mapped iso-surfaces, Journal of Applied Crystallography 39 (2006) 901–904.